Iranian Society of Acoustics and Vibration
The 13th ISAV2023 International Conference on Acoustics and Vibration
20, 21 Dec 2023 Tehran - Iran

# Fuzzy control of road excitation simulator by an electro-hydraulic actuator

Mohammad Javad Azizi [a*], Mehdi Mirzaei [b], Sadra Rafatnia [c]

[a] *Master Degree, Sahand University of Technology, Tabriz, 513351996, Iran.*
[b] *Professor, Sahand University of Technology, Tabriz, 513351996, Iran.*
[c] *Assistant Professor, Sahand University of Technology, Tabriz, 513351996, Iran.*
* *Corresponding author e-mail: mj_azizi400@sut.ac.ir*

## Abstract

Road excitation simulator is used to generate time-varying road irregularities applied to vehicle platform in a laboratory. This study deals with experimentally implementation of an electrohydraulic actuator control in a road excitations simulator. A fuzzy controller is designed based on the expert knowledge of the system, in which the output is measured using a linear variable differential transformer (LVDT). The fuzzy controller employs the Mamdani method structure to calculate the appropriate voltage of the electro-hydraulic directional valves for tracking the desired inputs for road excitations. Finally, the experimental results conducted on a fabricated platform of road simulator is given to illustrate the good performance of the proposed control scheme. The controller is implemented in the LabView interface, and the results of the proposed controller are compared with the conventional PID in different reference trajectories. The results indicate the accuracy and reliability of the proposed method in comparing with the conventional proportional-integral-derivative (PID) controller.

**Keywords**: Fuzzy controller; electro-hydraulic actuator; hydraulic valves; practical implementation.

## 1. Introduction

Nowadays, the demands of customers and the competitive environment between car manufacturers have increased the development of modern suspension systems in various kinds of passive, semi-active and active systems. The main feature of these systems is to adjust the suspension parameters for improvement of ride comfort and handling of vehicles in a wide range of road inputs [1-3]. To meet these objectives more closely, the designed suspension systems are required to be tested in the laboratory under various road irregularities.

Construction of the standard road profile is crucial for vehicle suspension systems as it forms the basis for understanding system behaviour, identifying the parameters and testing the performance of the designed system. In this regard, the use of electric motors [4-6], pneumatic actuators [7], electric actuators [8, 9] and hydraulic actuators [10, 11] are common in designing road simulators for suspension systems. Lin et al. [5] used a mesh rotating disc to design the road profile in their structure. This structure shows the ability to produce a road input in the form of two bumps. Mirzaei et al. [4] presented the ability of sinusoidal road inputs with constant amplitude and specific frequency spectrum using an electric motor. Akbari and Lohman [8] used a custom electric actuator to generate road input. In the studies mentioned above, a simple road input can be provided, and the problem of controller design is dropped for designing the desired road input.

It is found from the literature that the existing position control algorithms take different strategies. Gue et al. [12] proposed an extended state observer-based sliding mode controller for position control of an electro-hydraulic actuator. Chen et al [13] introduced a sliding mode controller with varying boundary layers for an electro-hydraulic position servo system. A nonlinear output feedback controller coupled with a high-gain observer was provided for an electro-hydraulic system [14]. Generally, the effectiveness of the model-based control methods reviewed above relies on accurate modeling of the system. In addition, due to the nonlinear full-order model of the hydraulic actuators, the order of system is increased, making the controller design difficult. Moreover, using extra sensors to measure full states of the system is not cost-effective. Model-free control methods such as proportional-derivative-integral (PID) controllers [15-17] and fuzzy controllers [18-20] are alternative approaches for position control of electro-hydraulic actuators. Wonohadidjojo et al. [18] proposed a fuzzy logic controller for an electro-hydraulic actuator. Chen et al. [19] used an integrated fuzzy controller to achieve a synchronous positioning objective for a dual-cylinder electro-hydraulic, lifting system with unbalanced loadings.

This study deals with the design and experimentally implementation of a Mamdani-based fuzzy logic controller for position control of the electro-hydraulic actuator to generate road profiles with different amplitudes and frequencies. In the mechanical structure of the road profile simulator, the shaft and the guide bush are used to produce vertical movement. Also, to compensate for the weight of the platform, and to prevent the increase in power consumption of the hydraulic system, a spring with a suitable stiffness is used. In the proposed structure, with the installation and calibration of a linear variable differential transformer (LVDT), the displacement information of the platform is measured. Then, in order to implement road profiles with different amplitudes and frequencies, a fuzzy controller is used to generate the appropriate voltage for the electro-hydraulic valve. The results obtained by the proposed strategy are compared with the other control strategies to show its effectiveness in controlling of electro-hydraulic actuator for providing different road profiles.

The paper is organized as follows: After Introduction, in the section 2, the overview of the road simulator system is presented. The kinetic model of the road profile simulator is illustrated in section 3. In the section 4, a fuzzy controller algorithm is developed and the PID controller as a conventional method is presented. The results of the practical implementation are discussed in section 5. Finally, the conclusion is given in the last section.

## 2. The overview of the road simulator system

Figure 1 depicts the structure of the road excitation simulator fabricated in the Mechatronics Laboratory of Sahand University of Technology (SUT). The road excitation simulator is controlled by an electro-hydraulic actuator. An OPKON LVDT sensor is attached to the platform to measure its displacement with a frequency of 100 Hz. A PCI NI-DAQ-6052 card is used for the serial connection between the platform and the computer, which receives data from the sensor and sends the control signals to the digital valve amplifier (DVA) card. In this structure, receiving, acquiring, and processing of data are performed by LabView software. After calculating the control signal, these signals are sent to the DVA card through serial connection. The DVA processes digital input signals with precision and sending analogue commands to a DSE5-C60 Duplomatic directional servo valve, regulating the precise direction of hydraulic fluid flow. Then, the electro-hydraulic actuator, in turn, translates these commands into mechanical motion, ensuring the accurate positioning of critical components.

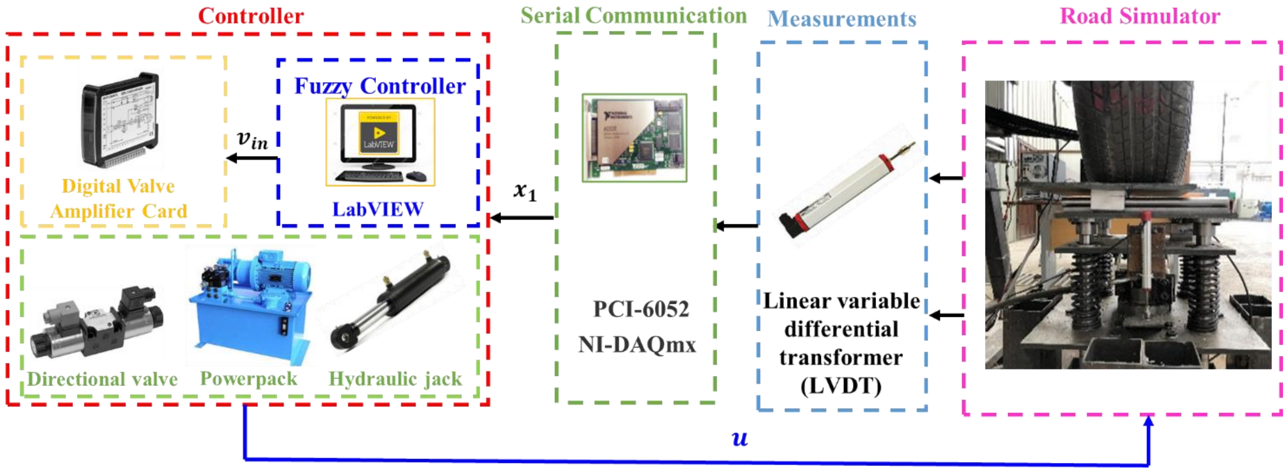


**Figure 1.** The overview of the proposed system.

## 3. Dynamic model of road simulation.

A schematic of the road simulator is shown in Fig. 2. This structure consists of an electro-hydraulic actuator and a set of springs for practical implementation. Based on Fig. 2, and considering the linear structure for the set of springs, the governing equations of the system in the state space form are derived as follows:

$$\dot{x}_1 = x_2, \tag{1}$$

$$\dot{x}_2 = \frac{K_r}{m_b} x_1 - \frac{u}{m_b}, \tag{2}$$

where $x_1$ is the road input and $x_2$ is the speed of the road input. Also, $K_r$ is the spring coefficient of the platform and $m_b$ is the total mass of a system. Also, the control input of the system is displayed with $u$.

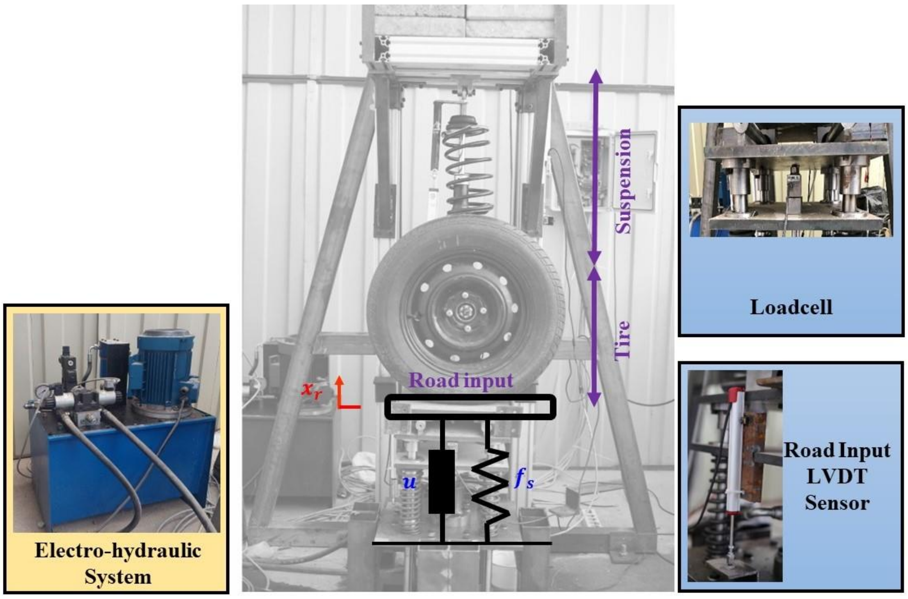


**Figure 2**. Dynamic diagram of road input generation.

In this study, the control force is produced by an electro-hydraulic actuator. According to Fig. 3, the actuator consists of a servo spool valve, activated by the voltage. The movement of the spool valve causes the flow of high-pressure fluid to pass to one of the upper or lower chambers of the cylinder, and the other side is connected to the oil tank. This flow creates a pressure difference on both sides of the piston. Therefore, the product of this pressure difference in the area of the piston is equal to the active force output from the actuator.

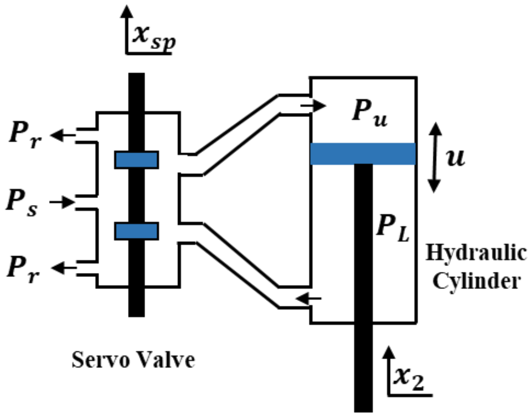


**Figure 3**. schematic of how the operator works

The equations related to the dynamics of the hydraulic actuator are as follows [20]:

$$u = AP_L \tag{3}$$

$$\frac{v_t}{4\beta}\dot{P}_L = Q_L - C_t P_L - A\mathrm{x}_2 \tag{4}$$

$$Q_L = C_d \omega x_v \mathrm{sgn}(P_s - P_L \mathrm{sgn}(x_v)) \sqrt{\frac{1}{p}|p_s - p_L \mathrm{sgn}(x_v)|} \tag{5}$$

In the above equations, $u$ is the force of the hydraulic actuator, $P_L$ is the pressure difference between the two sides of the piston, $A$ is the cross-sectional area of the piston, $v_t$ is the total volume of the actuator cylinder, $\beta$ is the effective bulk coefficient, $Q_L$ is the hydraulic flow rate, and $C_t$ is the total leakage coefficient of the piston, $C_d$ is the discharge coefficient, $\omega$ is the slope of its spool valve. $x_v$ is the displacement of the hydraulic valve, ρ is the density of the hydraulic fluid, Ps is the pressure created by the hydraulic pump. By defining parameters as follows:

$$\alpha = \frac{4\beta}{v_t}, \quad \beta = \alpha C_t, \quad \gamma = \alpha C_t \omega \sqrt{\frac{1}{\rho}} \tag{6}$$

and the combination of equations (4) and (6) will have:

$$\dot{P}_L = -\beta P_L - \alpha A\mathrm{x}_2 + \gamma x_v \mathrm{sgn}(P_s - P_L \mathrm{sgn}(x_v)) \sqrt{|P_s - P_L \mathrm{sgn}(x_v)|} \tag{7}$$

Also, the displacement value of the hydraulic valve spool, taking into account the time delay (τ), has the following relationship with the input voltage ($v_{in}$):

$$\dot{x}_v = \frac{1}{\tau}(-x_v + v_{in}) \tag{8}$$

With the aim of tracking the desired road profile by the actuator, two different control methods are used. In both control methods, the voltage of the actuator is defined as the control input.

In the following, at first, the PID controller is presented. Then, the proposed fuzzy controller is introduced.

# 4. Control system design

## 4.1. The proposed Fuzzy controller

In this section, the goal is to design a controller that the road profile simulator tracks the reference input. For this purpose, a structure based on Fig. 4 is presented. Based on this structure, the tracking error of the reference path and its derivative are considered as the input of the fuzzy system, and the voltage of the servo valves is considered as output of the controller. Based on Fig. 4, the control law can be derived as follows:

$$u(t) = K_c\left(K_p e(t) + K_d \Delta e(t)\right) \tag{9}$$

where *e(t)* and *Δe(t)* are the tracking error and the derivative of the tracking error, respectively. Note that, the difference between instance tracking error and delayed one is used as derivative of the tracking error in the LabView software. Also, the gains $Kp$ and $K_d$ are proportional and derivative gains, respectively, and $K_c$ is the gain coefficient for converting the output of the phased system to the voltage of the electrohydraulic valves.

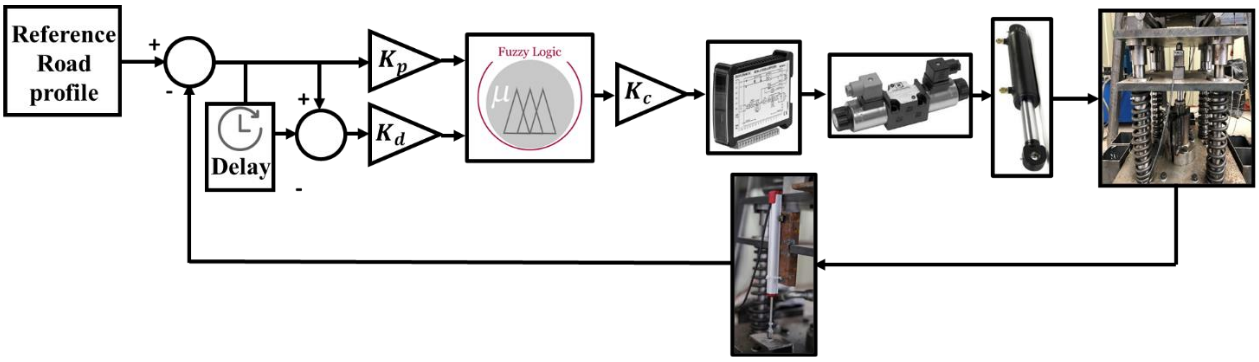


**Figure 4.** Fuzzy control system structure.

Membership functions of the fuzzy system for input and output variables are presented in Fig. 5. Based on Fig. 5, five language variables whose descriptions are provided in Table 1 are used. Also, 25 fuzzy rules according to Table 1 are used to create fuzzy rules for the purpose of tracking the reference road.

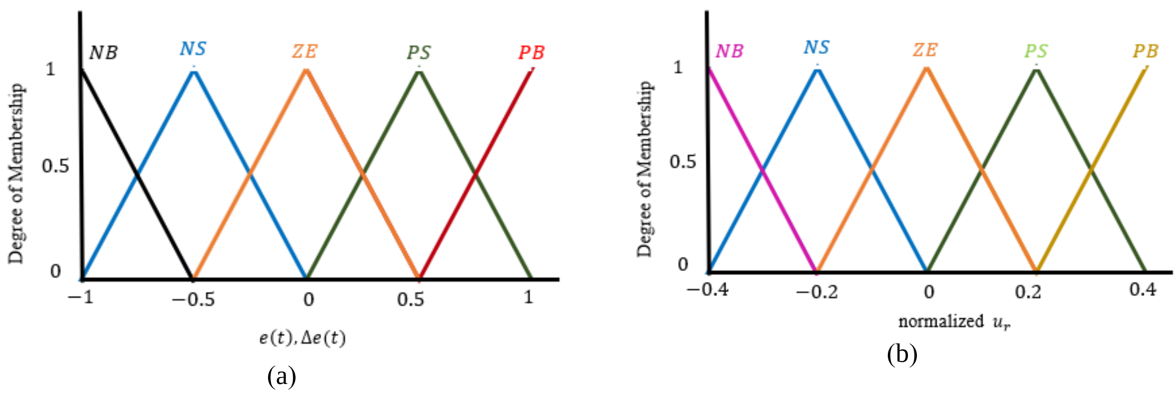


**Figure 5.** Diagram of how to create membership functions a) tracking error and its derivative (fuzzy system inputs) b) control force (fuzzy output)

**Table 1.** Introduction of membership functions

| $e(t), \Delta e(t)$ | **NB** | **NS** | **Z** | **PS** | **PB** |
|---|---|---|---|---|---|
| **NB** | PB | PB | PB | PS | ZE |
| **NS** | PB | PB | PS | ZE | NS |
| **ZE** | PB | PS | ZE | NS | NB |
| **PS** | PS | ZE | NS | NB | NB |
| **PB** | ZE | NS | NB | NB | NB |

## 4.2. PID controller

The PID controller is a widely used feedback control system for control of electro-hydraulic actuators [15-17]. According to Fig. 6, the PID controller is designed to regulate and stabilize systems by continuously adjusting an output based the difference between a desired road input and the measurement from LVDT. In this structure, the control signal is calculated as

$$u(t) = K_p e(t) + K_d \dot{e}(t) + K_i \int e(t)dt \tag{10}$$

where the tracking error denotes $e = x_{1d} - x_1$. The three components of the PID controller play distinct roles: $K_p e(t)$ is the proportional component and provides an immediate response to the current error, the integral component, $K_i \int e(t)dt$, eliminates any steady-state error by accumulating past errors, and the derivative component, $K_d \dot{e}(t)$, anticipates future error trends and counteracts them. By combining these components, a PID controller can achieve precise control.

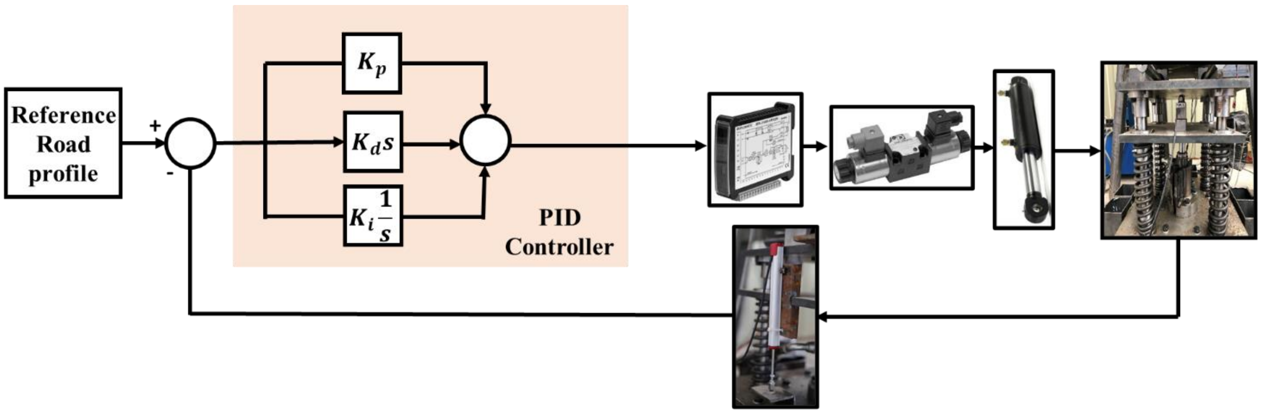


**Figure 6.** PID control system structure.

## 5. Results

In this section, the results related to the practical implementation of the proposed controller for input generation are presented. For the fuzzy control, the proportional gain coefficient of $Kp$=1 and the derivative gain coefficient of $K_d$=0.001 are selected. Also, the output conversion gain coefficient is selected according to the scale of production outputs as $Kc$=20. Note that, the maximum analogue signal that can be sent by the data card is 8 volts. This voltage is linearly converted to the supply voltage of the valves by the proportional valve card.

In the following, the results of the proposed controller are compared with the conventional PID in different harmonic reference trajectories. In the first result, a harmonic reference trajectory with amplitude 2 (cm) is used as the reference road input. Note that, the gain of the conventional PID is tuned by trial and error to have minimum tracking error. The comparison results between the proposed fuzzy controller and the conventional PID, shown in Fig. 7, indicate the similar performance of both controllers. Both controllers have a good performance in tracking the desired trajectory. It is necessary to mention that a saturation function is used in front of the control voltage input and the applied control voltage diagrams also show the control voltages in the range of 8 and -8 volts. Also, the control force provided by the jack is also presented in Fig. 6d. According to Fig. 6d, the control force is in the range of 200 N to produce the harmonic road inputs.

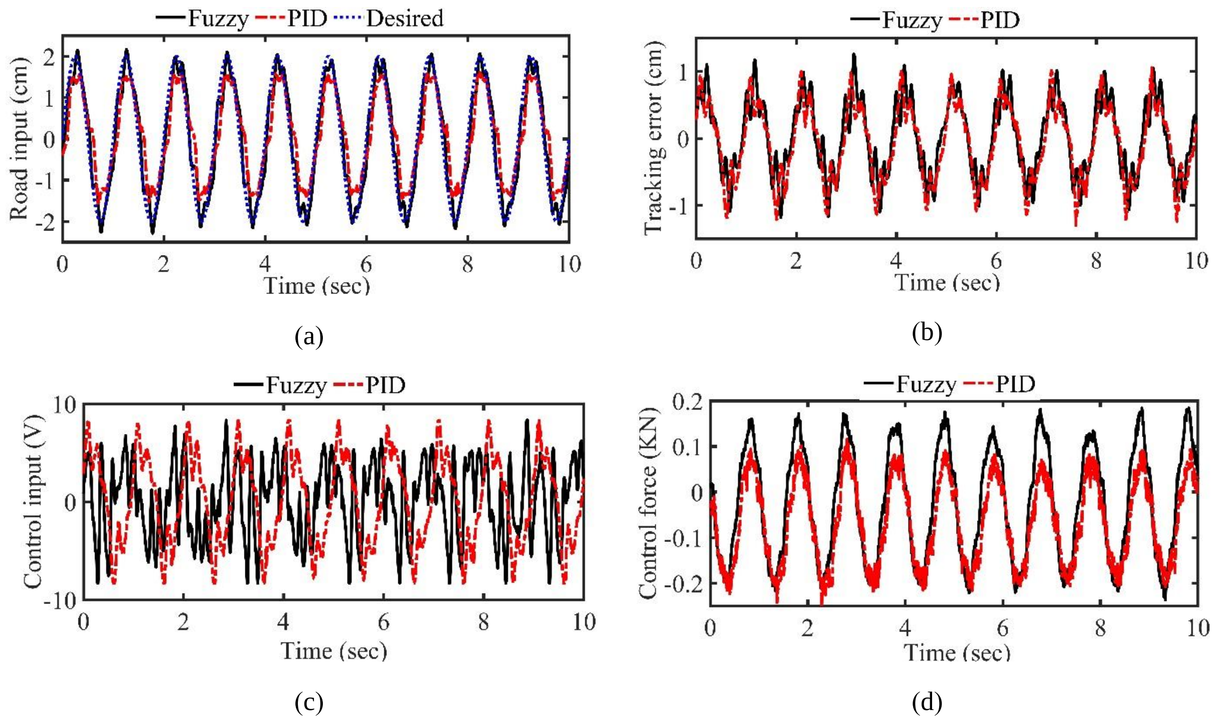


**Figure 7.** Test results for a range of 2 cm, a) Road input, b) Tracking error, c) Control input, d) control force.

In order to show the performance of the proposed controller in other trajectories, the response of the system for a harmonic trajectory with amplitude 3 (cm) is shown in Fig. 8. The results of the practical implementation of controllers for generating the road input indicate the lower tracking error of the proposed controller in tracking the reference path and generating the road input compared to the PID controller. This is for the reason that the proposed method, as an intelligent control method, uses the soft computing approach for calculation of the control input. However, the PID tries to track the reference trajectory with the gains calculated in the previous test.

To show the independency of the proposed control method in other trajectories, the results of both controllers are compared in different road trajectories. The comparative results for two periodic trajectories, shown in Figs. 9 and 10, indicate the higher accuracy of the proposed controller in comparison with the conventional PID controller. The proposed controller can handle the nonlinear systems with complex, vague, or imprecise dynamics. In addition, the proposed method requires less tuning effort and is useful when the reference input changes.

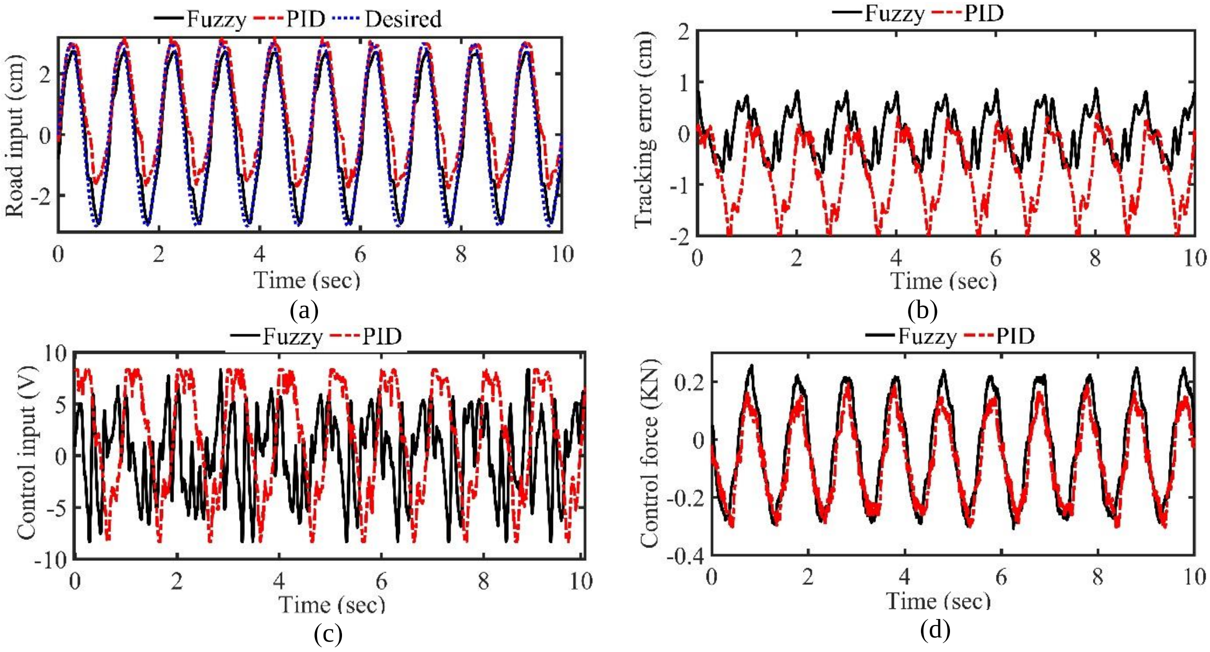


**Figure 8.** Test results for a range of 3 cm, a) Road input, b) Tracking error, c) Control input, d) control force.

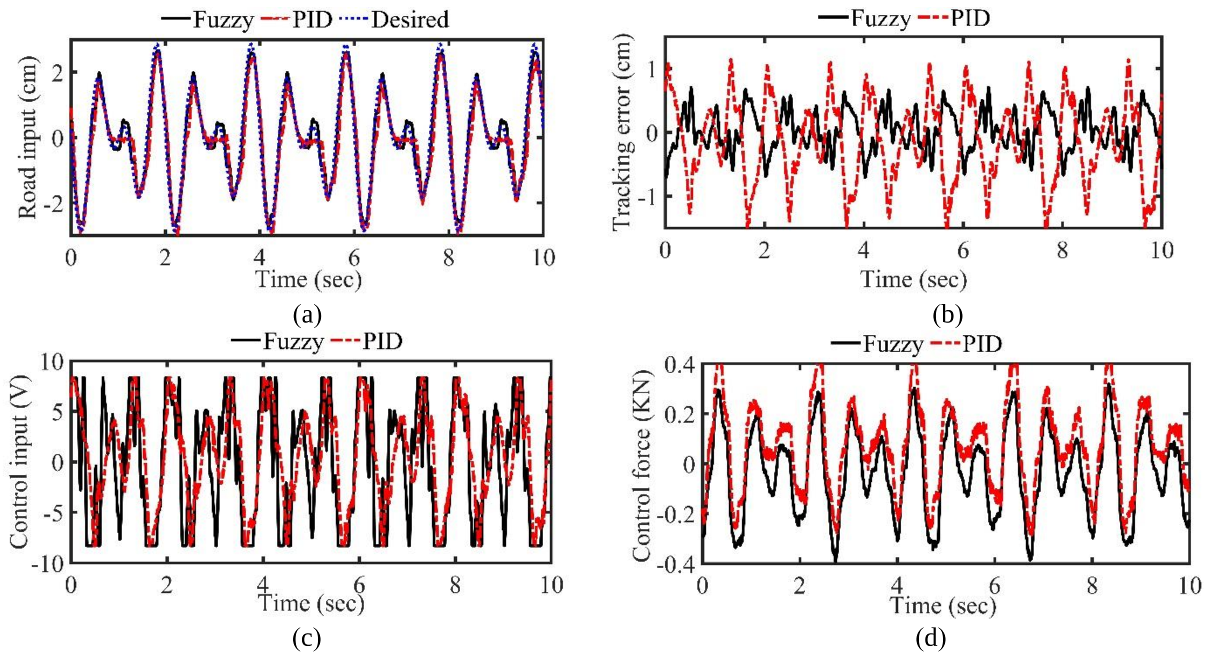


**Figure 9.** Test results for the first periodic reference road, a) Road input, b) Tracking error, c) Control input, d) control force.

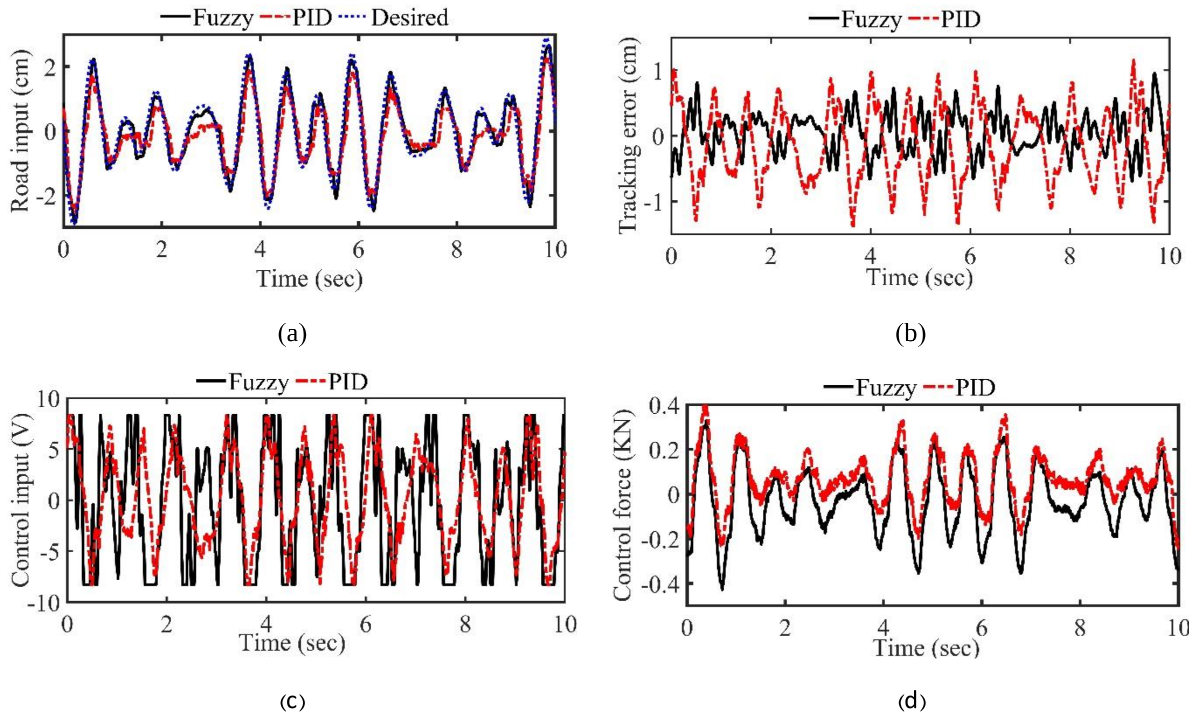


**Figure 10.** Test results for the second periodic reference road, a) Road input, b) Tracking error, c) Control input, d) control force.

## 6. Conclusion

In this research, a fuzzy controller is designed and experimentally implemented for a road profile simulator. The proposed controller uses the Mamdani logic to calculate the appropriate voltage of the electro-hydraulic actuator by using the measured data. The experimental results conducted on a fabricated platform of road simulator illustrate the good performance of the proposed control scheme. The results indicate more accurate and reliable responses for the proposed method in comparing with the conventional proportional-integral-derivative (PID) controller.

## REFERENCES

[1] Aghasizade, S., Mirzaei, M., & Rafatnia, S. (2018). Novel constrained control of active suspension system integrated with anti-lock braking system based on 14-degree of freedom vehicle model. *Proceedings of the Institution of Mechanical Engineers, Part K: Journal of Multi-body Dynamics*, *232*(4), 501-520.

[2] Aghasizade, S., Mirzaei, M., & Rafatnia, S. (2019). The effect of road quality on integrated control of active suspension and anti-lock braking systems. *AUT Journal of Mechanical Engineering*, *3*(1), 123-135.

[3] Abdi, B., Mirzaei, M., & Mojed Gharamaleki, R. (2018). A new approach to optimal control of nonlinear vehicle suspension system with input constraint. *Journal of vibration and control*, *24*(15), 3307-3320.

[4] Salmani Arani, M.M., Mirzaei, M., Akbari Alvanagh, A. and Aghasizade Shaarbaf, S., 2016. Identification of a nonlinear model for elements of a test rig of quarter car suspension system. *Modares Mechanical Engineering*, *15*(11), pp.136-142.

[5] Lin, J., Cheng, K. W. E., Zhang, Z., Cheung, N. C., & Xue, X. (2015). Adaptive sliding mode technique-based electromagnetic suspension system with linear switched reluctance actuator. IET Electric Power Applications, 9(1), 50-59.

[6] Simon, K. K., Syukri, H., Ilyas, R., & Onny, S. (2017). Pneumatic Actuator As Vertical Dynamic Load Simulator On The Suspension Mechanism Of A Quarter Vehicle Wheels. *ARPN Journal of Engineering and Applied Sciences*, *12*(23), 6975-6980.
[7] Koch, G., Pellegrini, E., Spirk, S., & Lohmann, B. (2010). Design and modeling of a quarter-vehicle test rig for active suspension control. Lehrstuhl für Regelungstechnik.
[8] Akbari, A., & Lohmann, B. (2010). Output feedback H∞/GH 2 preview control of active vehicle suspensions: a comparison study of LQG preview. *Vehicle System Dynamics*, *48*(12), 1475-1494.
[9] Chen, K., & Beale, D. G. (2003). Base dynamic parameter estimation of a MacPherson suspension mechanism. Vehicle System Dynamics, 39(3), 227-244.
[10] Ledwidge, J. (1995). System identification and parameter estimation of a motorcycle suspension system (Doctoral dissertation, Dublin City University).
[11] Chindamo, D., Gadola, M., Armellin, D., & Marchesin, F. (2017). Design of a road simulator for motorcycle applications. *Applied Sciences*, *7*(12), 1220.
[12] Guo, K., Wei, J., Fang, J., Feng, R., & Wang, X. (2015). Position tracking control of electro-hydraulic single-rod actuator based on an extended disturbance observer. *Mechatronics*, *27*, 47-56.
[13] Chen, H. M., Renn, J. C., & Su, J. P. (2005). Sliding mode control with varying boundary layers for an electro-hydraulic position servo system. *The International Journal of Advanced Manufacturing Technology*, *26*, 117-123.
[14] Kim, W., Won, D., Shin, D., & Chung, C. C. (2012). Output feedback nonlinear control for electro-hydraulic systems. *Mechatronics*, *22*(6), 766-777.
[15] Tajjudin, M., Ishak, N., Ismail, H., Rahiman, M. H. F., & Adnan, R. (2011, June). Optimized PID control using Nelder-Mead method for electro-hydraulic actuator systems. In *2011 IEEE Control and System Graduate Research Colloquium* (pp. 90-93). IEEE.
[16] Elbayomy, K. M., Zongxia, J., & Huaqing, Z. (2008). PID controller optimization by GA and its performances on the electro-hydraulic servo control system. *Chinese Journal of Aeronautics*, *21*(4), 378-384.
[17] Tony Thomas, A., Parameshwaran, R., Sathiyavathi, S., & Vimala Starbino, A. (2022). Improved position tracking performance of electro hydraulic actuator using PID and sliding mode controller. *IETE Journal of Research*, *68*(3), 1683-1695.
[18] Wonohadidjojo, D. M., Kothapalli, G., & Hassan, M. Y. (2013). Position control of electro-hydraulic actuator system using fuzzy logic controller optimized by particle swarm optimization. *International Journal of Automation and Computing*, *10*, 181-193.
[19] Chen, C. Y., Liu, L. Q., Cheng, C. C., & Chiu, G. T. C. (2008). Fuzzy controller design for synchronous motion in a dual-cylinder electro-hydraulic system. *Control Engineering Practice*, *16*(6), 658-673.
[20] Abdi, B., Mirzaei, M., Rafatnia, S., & Akbari Alvanagh, A. (2017). Analytical Design of Constrained Nonlinear Optimal Controller for Vehicle Active Suspension System considering the Limitation of Hydraulic Actuator. *Journal of Control*, *11*(3), 25-34.